AD_____

Award Number: W81XWH-11-1-0221

TITLE: Biomarkers for Pulmonary Injury Following Deployment

PRINCIPAL INVESTIGATOR: Richard Gelinas, Ph.D.
Kai Wang, Ph.D.
Joseph Brown, Ph.D.

CONTRACTING ORGANIZATION: Institute for Systems Biology
Seattle, WA 98103

REPORT DATE: February 2013

TYPE OF REPORT: Annual

PREPARED FOR: U.S. Army Medical Research and Materiel Command
Fort Detrick, Maryland 21702-5012

REPORT DOCUMENTATION PAGE

Form Approved
OMB No. 0704-0188

1. REPORT DATE *(DD-MM-YYYY)*	2. REPORT TYPE	3. DATES COVERED *(From - To)*
February 2013	Annual	1 February 2012 - 31 January 2013

4. TITLE AND SUBTITLE
Biomarkers for Pulmonary Injury Following Deployment

5a. CONTRACT NUMBER

5b. GRANT NUMBER
W81XWH-11-1-0221

5c. PROGRAM ELEMENT NUMBER

6. AUTHOR(S)
Dr. Richard Gelinas; Dr. Kai Wang; Dr. Joseph Brown

E-Mail: rgelinas@systemsbiology.org

5d. PROJECT NUMBER

5e. TASK NUMBER

5f. WORK UNIT NUMBER

7. PERFORMING ORGANIZATION NAME(S) AND ADDRESS(ES)
Institute for Systems Biology
Seattle, WA 98103

8. PERFORMING ORGANIZATION REPORT NUMBER

9. SPONSORING / MONITORING AGENCY NAME(S) AND ADDRESS(ES)
U.S. Army Medical Research and Materiel Command
Fort Detrick, Maryland 21702-5012

10. SPONSOR/MONITOR'S ACRONYM(S)

11. SPONSOR/MONITOR'S REPORT NUMBER(S)

12. DISTRIBUTION / AVAILABILITY STATEMENT
Approved for Public Release; Distribution Unlimited

13. SUPPLEMENTARY NOTES

14. ABSTRACT

To understand the risks of lung disease faced by soldiers, USACEHR has studied a rat model of lung disease after instillation of dust or silica. After exposure, lung pathology was measured and we identified the proteins and microRNAs that were released into the lung lavage fluid at different times after exposure so that the markers could be correlated with the observed pathology. In this model silica affected the lung more than dust from Iraq, and we reported the proteins and microRNAs we found in lavage fluid after either treatment. The candidate biomarkers we found came from lavage fluid which is relatively accessible. The markers we found can now be compared to markers from human clinical specimens. This work is underway via a collaboration with the STAMPEDE project at BAMC.

15. SUBJECT TERMS
Dust instillation/lung injury/protein biomarker/microRNA biomarker/bronchial lavage fluid

16. SECURITY CLASSIFICATION OF:			17. LIMITATION OF ABSTRACT	18. NUMBER OF PAGES	19a. NAME OF RESPONSIBLE PERSON
a. REPORT	b. ABSTRACT	c. THIS PAGE			USAMRMC
U	U	U	UU	27	19b. TELEPHONE NUMBER *(include area code)*

Table of Contents

Page

Introduction & Overview

Our overall goal in this Contract is to work with USACEHR to understand whether US soldiers were at risk for acute or chronic breathing disorders after service in SW Asia. As one approach to this problem, USACEHR has coordinated research on a preclinical rat model of lung pathology secondary to dust instillation. In one study, dust collected from the air at Camp Victory, Iraq (IR8 dust) or silica (as a positive control) was instilled into the lungs of rats. Lung tissue, bronchial alveolar lavage fluid (BALF), and blood serum were collected at various times thereafter. Lung tissue from animals treated with IR8 dust was studied for changes by veterinary pathologists, while microRNAs (miRNA) or proteins in BALF and miRNAs in serum were profiled at ISB and PNNL which was supported by this Contract.

MiRNAs or proteins that were generally associated with different lung pathologies were revealed by comparing profiles from animals that were treated with IR8 dust with samples from saline-treated lungs (negative control group) or silica (positive control group). According to the final pathology report by Green and Harley[22] while silica was "…the most pro-inflammatory of the dusts and caused the greatest proliferative and dysplastic changes in epithelial cells…" the IR8 dust caused only mild inflammatory or proliferative changes throughout the study period. In a subsequent study, two different dust samples were tested by the same protocol and also showed scant pathology. With some confidence we report the differentially expressed miRNAs and proteins that were found in the BALF after treatment with IR8 dust or silica, relative to saline. We also studied preliminary profiles for miRNA in the serum samples, but low RNA concentrations as well as hemolysis during sample collection makes these results quite variable and thus less informative, as we discussed in last year's report.

Here we present our final lists of proteins and miRNAs derived from the rat model. We have now independently verified many of the pathology-associated miRNAs we reported last year by studying lung tissue. We did this by profiling miRNAs extracted from thin sections cut from the same formalin-fixed, paraffin-embedded lung tissue samples that were studied by the veterinary pathologists cited above. The list of verified candidate miRNA biomarkers from this preclinical model can now be compared with the literature. Several miRNAs we detected have been linked to particular biological processes such as inflammation or fibrosis which coincide with the pathology findings of this rat model. In some cases, miRNAs we detected in these studies have also been reported as possible serum biomarkers for non-small cell lung carcinoma or prostate cancer. Thus the differentially expressed proteins and miRNAs derived from the rat model are ready to be verified with human clinical studies.

To begin translational studies, we are now collaborating with Dr. Michael Morris from the Brooke Army Medical Center who has sent us clinical samples from 48 active duty soldiers with dyspnea who enrolled in Dr. Morris' study called STAMPEDE. Working with USACEHR we extended the term of the current Contract to work with Dr. Morris. Protein profiling on BALF and urine is now in progress by Dr. Brown at PNNL. MiRNA profiling on urine, BALF, and serum is in progress at ISB by Drs. Gelinas and Wang. Unlike the rat model that was based on a single exposure to a defined agent (dust or silica) we expect more diverse underlying pathologies or diseases in the STAMPEDE cohort. But we are confident that our informatics tools can detect multiple disease signatures should they exist in the data, which we can then relate to each soldier's clinical findings by working closely with Dr. Morris.

Should distinct protein- or miRNA signatures that are linked to particular underlying lung diseases emerge from these human studies we will compare them to the findings from the dust instillation rodent model. This would represent real progress towards the goal of defining panels of candidate biomarkers for certain lung diseases that can be studied in easily obtained fluids. Moreover, the

miRNA and protein profiles from BALF secondary to dust and silica exposure have never been reported and thus represent an important contribution to the literature on inhalation toxicity. The ultimate goal will be to describe valid markers for lung disease diagnosis, disease stratification, progression, and response to drug therapy which would provide valuable diagnostic information in the lung clinic.

Candidate protein markers from BALF: introduction and experimental approach

An abbreviated description of the proteomics analysis is presented. For a detailed description of results and methods, please refer to the 2012 Annual Report for this contract. Rat BALF samples were denatured, digested, and desalted prior to liquid chromatography-mass spectrometry (LC-MS)-based proteomics analyses[1,2]. A foundational peptide database was generated[3] by pooling a subset of the peptides across time and biological replicates, which resulted in three pools: control (saline), dust, and silica. Pools were fractionated, using high-pH to reduce peptide complexity. Twenty-four individual fractions within each treatment condition were analyzed using an LTQ mass spectrometer (Thermo Scientific, Waltham, MA), and the peptide information (e.g., mass, normalized elution times) derived from the resulting 72 reversed phase LC-tandem MS (LC-MS/MS) analyses were stored in a reference database used for identifying peptides in subsequent high throughput, high resolution LC-MS analyses. 107 individual lung fluid samples were then analyzed using an LTQ-Orbitrap mass spectrometer (Thermo Scientific, Waltham, MA)[1]. Peptides identified from the resulting LC-MS/MS spectra were then used to augment the reference database. High-resolution MS spectra from these 107 samples were aligned to the database for quantitative proteomics analysis.

LC-MS/MS spectra were searched and annotated using SEQUEST and the *Rattus norvegicus* SwissProt database that contains 35,683 unique protein sequences, and parameters[1,2]. Peptides identified from SEQUEST search results were verified using the software package MS-GeneratingFunction (MSGF) with a spectrum probability score $\leq$ 1E-8[4], which resulted in a false discovery rate (FDR) of <5%. High-resolution reversed phase LC-MS spectra were deconvoluted using Decon2LS[5], and aligned to the peptide database using in-house software VIPER[6]. Highly confident peptide assignments were determined using a FDR threshold < 10% and a uniqueness probability > 0.5[7]. Redundant protein assignments (i.e. proteins identified by a common set of peptides such as isoforms and other closely related proteins), were consolidated using ProteinProphet[8], which resulted in what will further be referred to as “ProteinGroups”. ProteinGroups identified by a single unique peptide sequence were removed to increase confidence in ProteinGroup assignments. Peptide relative abundance values were normalized, outliers were removed, and then consolidated into ProteinGroup abundance scores using RRollup, with peptides that passed Grubb’s filters and $P \leq 0.059$. A 2-way ANOVA was performed on the ProteinGroups to determine the significance of difference and interactions between treatment and day post-treatment (pt) relative to controls. *P*-values from the 2-way ANOVA were adjusted for FDR by Benjamini-Hochberg’s correction. ProteinGroups were considered significantly different from control with $P \leq 0.05$. For more details, including visualization of the data with heatmaps, and the derivation of the Gene Ontogeny (GO) and GOSlim terms used in Tables 1-3, please see the 2012 Annual Report.

Protein markers from BALF: Results and Discussion

This proteomics analysis measured the relative abundance of 9195 peptides in rat BALF that corresponded to 588 ProteinGroups. Corrected 2-way ANOVA analyses identified 13 and 46 proteins that showed a significant difference ($P \leq 0.05$) by dust and silica, respectively. Three proteins were significantly different in both dust and silica treatments. While silica produced a considerably larger response than dust, dust and silica elicited relatively distinct pulmonary proteome response profiles in rat lung fluid. Proteins that exhibited a significant difference in

relative abundance in lung fluid exclusively following IR8 dust treatment over time are listed in Table 1; exclusively following silica treatment over time, in Table 2; and upon either dust or silica treatment over time, in Table 3.

Table 1. Proteins that showed a significant difference in relative abundance in lung fluid exclusively following IR8 dust treatment over time.

SwissProt	*Symbol*	*GO Term Name*	*GOSlim Description*
S10AB_RAT	*S100a11*	*Calcium ion binding*	*Cellular component*
H2A1_RAT	*Hist2h2aa3*	*DNA binding*	*Cellular component assembly*
D4A3X4_RAT			
LDHA_RAT	*Ldha*	*Response to hypoxia*	*Response to stress*
CADH1_RAT	*Cdh1*	*Response to toxin*	*Cell junction organization*
A1A5R2_RAT			
MDHM_RAT	*Mdh2*	*Tricarboxylic acid cycle*	*Carbohydrate metabolic process*
CYTC_RAT	*Cst3*	*Response to hypoxia*	*Lysosome*
KCRB_RAT	*Ckb*	*Creatine kinase activity*	*Small molecule metabolic process*
HBA_RAT	*Hba-a2*	*Oxygen transport*	*Circulatory system process*

Table 2. Proteins that showed a significant difference in relative abundance in lung fluid exclusively following silica treatment over time.

SwissProt	Symbol	GO Term Name	GOSlim Description
D4AD25_RAT			
LPLC1_RAT	*RGD1563047*	*Lipid binding*	*Extracellular region*
D4A400_RAT			
A1AT_RAT	*Serpina1*	*Inflammatory response*	*Response to stress*
D3ZD91_RAT			
CO4_RAT	*C4b*	*Inflammatory response*	*Response to stress*
CHIA_RAT	*Chia*	*Chitinase activity*	*Response to stress*
WFDC2_RAT	*Wfdc2*	*Peptidase inhibitor activity*	*Extracellular component*
F1LMJ9_RAT	*Eprs*		
HS71L_RAT	*Hspa1l*		
MINP1_RAT	*Minpp1*	*Phosphatidylinositol-mediated signaling*	*Signal transduction*
F1LWD0_RAT			
H2B1_RAT	*LOC684797*	*DNA binding*	*Cellular component assembly*
PON1_RAT	*Pon1*	*Response to toxin*	*Lipid metabolic process*
D4A2G2_RAT			
OSTP_RAT	*Spp1*	*Inflammatory response*	*Response to injury*
GFAP_RAT	*Gfap*	*Response to wounding*	*Response to stress*
A1M_RAT	*Pzp*	*Endopeptidase inhibitor activity*	*Extracellular space*
PSA2_RAT	*Psma2*		
Q9QX71_RAT			
Q5XJW6_RAT			
TCTP_RAT	*Tpt1*	*Cell proliferation*	*Intracellular*
CATD_RAT	*Ctsd*	*Lysosome*	*Vacuole*
D4ABW1_RAT			
D3ZE08_RAT			
CYBP_RAT	*Cacybp*	*Cellular response to calcium ion*	*Nucleus*
PRDX2_RAT	*Prdx2*	*Response to oxidative stress*	*Response to stress*
HBB1_RAT	*LOC100134871*	*Oxygen transport*	*Circulatory system process*
ILEUA_RAT	*Serpinb1a*	*Peptidase inhibitor activity*	*Extracellular region*
TRFE_RAT	*Tf*	*Response to hypoxia*	*Response to stress*

CD59_RAT	*Cd59*	*Complement binding (inhibits MAC)*	*Extracellular space*
SFTPA_RAT	*Sftpa1*	*Response to hypoxia (and IL-6)*	*Response to stress*
THRB_RAT	*F2*	*Fibrinolysis*	*Response to stress*
PLMN_RAT	*Plg*	*Fibrinolysis*	*Response to stress*
D4A183_RAT			
ARK72_RAT	*Akr7a2*	*Oxidoreductase activity*	*Mitochondrion*
EF1G_RAT	*Eef1g*	*Translational elongation*	*Translation*
D3ZJF8_RAT			
VIME_RAT	*Vim*	*Intermediate filament*	*Cytoskeleton*
GRAB_RAT	*Gzmb*	*Proteolysis*	*Apoptotic process*
TBB2A_RAT	*Tubb2a*	*Microtubule*	*Cytoskeleton*
S14L2_RAT	*Sec14l2*	*Enzyme activator activity*	*Intracellular*
ANXA4_RAT	*Anxa4*	*Exocytosis*	*Vesicle-mediated transport*

Table 3. Proteins that showed a significant difference in lung fluid by dust and by silica treatment over time.

SwissProt	***Symbol***	***GO Term Name***	***GOSlim Description***
APOE_RAT	*Apoe*	*Response to oxidative stress*	*Response to stress*
CATB_RAT	*Ctsb*	*DNA binding*	*Cellular component assembly*
Q68FT8_RAT			

Proteins from BALF as potential biomarkers of lung pathology

This study identified a significant increase in the presence of lactate dehydrogenase (Ldha) in rat lung fluid exclusively upon dust treatment (Table 1). The protein also showed higher abundance in the lung fluid of rats exposed to silica, but not to significant levels. Ldha activity is a commonly assessed biomarker in lung fluid for determining nonspecific damage to the airways[12,13]. The Ldha enzyme is typically cytoplasmic, but is excreted by lung cells during disturbances to cellular integrity resulting from pathological conditions[14].

As described in the pathology report[22], the pulmonary histology showed an increased macrophage response to both dust and silica treatments. Alveolar macrophages are a considerable source of pulmonary inflammation in lung disease largely because they produce a number of proteases, including cathepsins that damage lung tissue[15]. Cathepsins are inhibited by cystatin C. While our proteomics analyses identified a significant increase in cathepsin B by dust and silica in the latest time point (Table 3) and cathepsin D exclusively by silica treatment (Table 2), we also measured a decrease in cystatin C (Table 1).

Cigarette smoke induces oxidative stress that can accelerate epithelial cell senescence that results in chronic obstructive pulmonary disease (COPD) pathogenesis. Creatine kinase (Ckb) is a constitutive enzyme that regulates cell senescence and is decreased in cigarette smoke-

induced stress[16]. Ckb was also significantly decreased in our study within 7 days following treatment with dust.

Meloni et al. previously investigated potential biomarkers in lung fluid of lung transplant recipients to predict the development of bronchiolitis obliterans syndrome (BOS) versus long-term survival (LTR)[17]. Among 11 differentially expressed proteins between BOS and LTR, their study identified two factors that showed consistent differences in expression relating to long-term lung transplant outcome: peroxiredoxin II (PRXII) that was exclusively expressed in BOS, and surfactant protein A (SP-A) that consistently showed lower expression in BOS patients compared to stable LTRs.

Both Prdx2 and Sftpa1 exhibited significantly different levels exclusively in rats exposed to silica compared to the control (Table 2). Similar to abundance levels of PRXII and SP-A that distinguish between BOS and LTR in lung transplant recipients, Prdx2 showed elevated levels of expression by 120 days p.t. in the lung fluid of rats exposed to silica, while Sftpa1 was persistently low at the four time points studied. Expression profiles of Prdx2 and Sftpa1 may be diagnostic signatures of chronic and progressive pulmonary inflammation. Since one is elevated and the other declines, they also represent a 'top scoring pair' with potentially high information content as biomarkers[10]. Furthermore, Sftpa1 is an important regulator of the pulmonary host defense and inflammatory response, and has been shown to down-regulate several pro-inflammatory cytokines, including IL-6 and TNFα[18]. The decrease in Sftpa1 abundance could be a nonspecific marker of pulmonary inflammation occurring in the lung fluid of silica-treated rats.

In our study, osteopontin (Spp1), a cytokine that is secreted into the pulmonary space by a variety of environmental toxins and treatment insults, showed a significant increase in lung fluid of rats treated with silica (Table 2). The presence of this cytokine has been implicated in a number of lung pathologies, including particle-lung disease[19], pulmonary fibrosis[20], and COPD[21].

Proteomics: Concluding Remarks

This analysis produced a comprehensive peptide reference database and a measure of relative abundance for 9195 peptides that correspond to 588 ProteinGroups. Overall, this approach provided a broad view of the rat BALF proteome in control rats and those treated with IR8 dust and silica. In addition, statistical analysis filtered this list of ProteinGroups to focus in on a small group that demonstrated relatively large changes in abundance. While silica induced the greatest response in BALF, proteomics analysis detected a signature response to dust that was distinct from the response to silica. The list of significantly different ProteinGroups represents potential candidates for further targeted, mechanistic studies to determine causal versus effect of response. As Tables 1-3 show, a large number of significantly different ProteinGroups are related to oxidative stress and the inflammatory response which corresponds with the pathology noted from the histology.

While peptide centric proteomics analysis provides information regarding proteins present in a sample, the approach is not without limitations. For example, this type of approach provides only limited information regarding post-translational modified proteins that are important regulators of protein localization and activation. With the proteomic approach using in this study, modifications of interest must be specified before a spectra search is initiated. Furthermore, the stoichiometry of some post-translational modifications can be so low as to require sample enrichment to promote detection. In contrast, oxidative modifications in pulmonary proteins are generally widespread, and can be detected within a given parameter space. Given the large number of ProteinGroups involved in oxidative stress (Tables 1-3) that showed significant difference in relative abundance in BALF, future analyses can target these types of oxidative modifications.

Overall, the study identified significant changes in several proteins in the BALF of rats exposed to either IR8 dust or silica that are involved in the response to stress, hypoxia, and inflammation. The proteomic response to dust was not as severe as the response to silica, which corresponds to the histological reports; however, dust produced a distinct proteomic signature from that of silica. A subset of each response showed similarities with pulmonary inflammatory responses observed in COPD, BOS in lung transplant patients, pulmonary fibrosis, and particle-lung disease. While the response proteins overlapping with these pathologies may represent nonspecific markers of pulmonary inflammation, the complete response profile can be used in future targeted studies (e.g., using single-reaction monitoring or enzyme-linked immunoassays) to develop and define unique bio-signatures specific to a particulate-induced lung disease.

A common characteristic of pulmonary silica treatment is inflammation. This inflammation is primarily mediated by alveolar macrophages, which produce a vast arsenal of proteases including cathepsins. Cathepsin activity can be regulated by cystatin C to control and mitigate the effects of inflammation. While the formal histology reports from the dust instillation model[22] indicated increased macrophage response in the lungs of rats exposed to both IR8 dust and silica treatments, proteome measurements of the BAL fluids from these rats measured an increase in cathepsin B and a decrease in cystatin C abundances. These results suggest that the pulmonary inflammation observed in lungs from these rats is primarily mediated by the unchecked cathepsin B production by activated alveolar macrophages.

High-resolution LC-MS(/MS)-based multidimensional proteome analysis identified a number of proteins that showed a significant difference over time between IR8 dust and silica treatments, and are involved in pulmonary pathology. These proteins, including Ldha, Ckb, Prdx2, and Sftpa1, show interesting expression profiles over time in the BAL fluid of the treated rats. The proteomic results have identified a number of ProteinGroups that have previously been linked to other pulmonary disorders and correspond with histological observations. The proteins and ProteinGroups identified from this pre-clinical model represent candidate biomarkers that are ready for comparison to the proteins in clinical samples from the STAMPEDE cohort.

Candidate miRNA markers from lung: validation of BALF miRNAs

BALF fluid and blood serum were recovered at the time of sacrifice of the rats that were part of the dust instillation studies designed by USACHER and carried out by a team at NIOSH. These samples were obtained both from a first study in which ambient air dust from Camp Victory, Iraq (abbreviated IR8) was instilled into the lungs of rats. Saline was instilled in other animals as a negative control and silica was instilled as a positive control. BALF and serum were also obtained from a subsequent study in which a different sample of dust from Iraq (abbreviated IR9) and a sample of urban dust collected in the United States (NIST dust) were instilled the lungs of rats, along with saline as above. MiRNAs from BALF and serum associated with the dusts or silica were presented in the 2012 Annual Report, along with details of quantitation by qPCR or hybridization. The principle focus of this report is the validation of the results from BALF by profiling lung tissue samples.

To validate our findings of pulmonary markers in lavage fluid or serum from rats that were exposed to dust or silica, we profiled miRNAs from lung tissue. We were able to isolate sufficient RNA from thin sections cut from formalin-fixed, paraffin-embedded lung tissue so that the miRNA fraction could be profiled by hybridization. We previously reported the profiles of differentially expressed proteins or miRNAs that were present in the lavage fluid of rats that were treated with IR8 dust or silica in USACEHR's study 1. After lavage, the lungs from these animals were dissected and prepared for histologic examination. Veterinary pathologists examined the slides and developed their assessments of the pathologic changes in the ultra-structure of the lung. The pathology findings were reported to USACEHR22 and specific pathology findings remain

traceable to particular blocks. We requested access to the blocks of formalin-fixed, paraffin embedded lung tissue and requested that additional sections be cut and sent to us for isolation of RNA and miRNA profiling studies.

We were able to isolate sufficient total cell RNA from thin sections to profile miRNAs by hybridization (the NanoString method). We asked if any of the miRNAs that were found in BALF were also differentially expressed in lung tissue. Indeed, several miRNAs found in BALF were independently detected in all lung tissue samples from animals exposed to silica for 30 and 60 days. These miRNAs were among a core group of differentially expressed species found in lung and BALF, induced by either dust or silica, after 1 to 2 months of exposure. Several of these miRNAs have been associated with inflammatory and fibrotic lung processes as well as other disorders.

Profiling miRNA from lung tissue-Methods

Five micron sections were cut from a set of formalin fixed, paraffin embedded lung tissue specimens in standard blocks. The blocks, all from study 1, were selected from rats that were exposed to 10 mg/kg silica for 30 days or 60 days along with the corresponding controls as summarized in Table 4.

Table 4. Source of lung samples for miRNA profiling

Experimental treatment (Iraq 1 study)	Thin sections cut from the indicated no. of blocks of lung tissue; one block per rat	Average RNA concentration, ng/ml, (40 ul total volume recovered)
Silica, 10 mg/kg, 30 day exposure	5	35
Controls for above	5	28
Silica, 10 mg/kg, 60 day exposure	4	26
Controls for above	3	12

Thin sections were trimmed of excess paraffin with a razor and the fixed lung tissue from 2 or 3 sections was placed in a tube. RNA including low mw RNA was isolated by using the miRNeasy FFPE kit (Qiagen, Cat. No. 217504). The yield of RNA was measured by asbsorption at 260 nm (NanoDrop Spectrophotometer ND-1000) and rat miRNAs were profiled by the Rat miRNA expression assay kit (NanoString Technologies, Seattle WA). This rat miRNA profiling system was capable of detecting 423 discrete species from miRBase 17. We followed the NanoString protocol except that we used twice as much total cell RNA as suggested (200 ng rather than 100 ng). The processing was completed using the nCounter Prep Station and the nCounter Digital analyzer as recommended by NanoString.

Two slightly different data reduction methods were used. For a preliminary view of the miRNAs that changed in abundance after exposure to silica, raw molecular counts were normalized by multiplying each value by mean of the internal control mRNAs that were measured in same tube (ActB, B2M, GapdH, Rpl19). Next, average scores for each miRNA species were calculated within the control and experimental groups. Then the mean control values for each miRNA were plotted against the corresponding experimental values for both the 30day and the 60 day studies. This analysis revealed miRNAs with strong differential expression. Since biological replicates were

profiled as shown in Table 4, p values were calculated via Welch's T-test applied between the control and silica-treated groups. The data could then be filtered by both the degree of differential expression (greater than or equal to 1.7-fold) along with the p value (less than or equal to 0.05) as explicit criteria of significance.

Profiling miRNA from lung tissue-Results

In this pilot study we profiled miRNAs from formalin-fixed, paraffin-embedded lung tissue by extracting RNA from thin sections cut from the blocks of study 1. Sections from these blocks had already been examined by the veterinary pathologists, and the results from each block could in principle be linked to the existing assessments of lung structure and the nature of any pathology. A rapid semi-quantitative assessment of the data was obtained by plotting the expression of a given miRNA from a silica treated lung as a function of the controls. Working in Excel, after normalizing and combining the values for lung miRNAs from the animals in the treatment groups given in Table 4, we plotted control expression (y-axis) as a function of the experimental expression (x-axis) for all miRNAs as shown in Figure 1. MiRNA-21 and 146b were differentially expressed in the lung tissue in rats after 30 days of exposure to 10 mg silica/kg (Fig. 1 A). These two miRNAs were detected again after 60 days of exposure (Fig. 1B). The fact that we could detect these miRNAs independently as being up-regulated in both the 30 day and 60 day groups strengthens the validity of the observation.

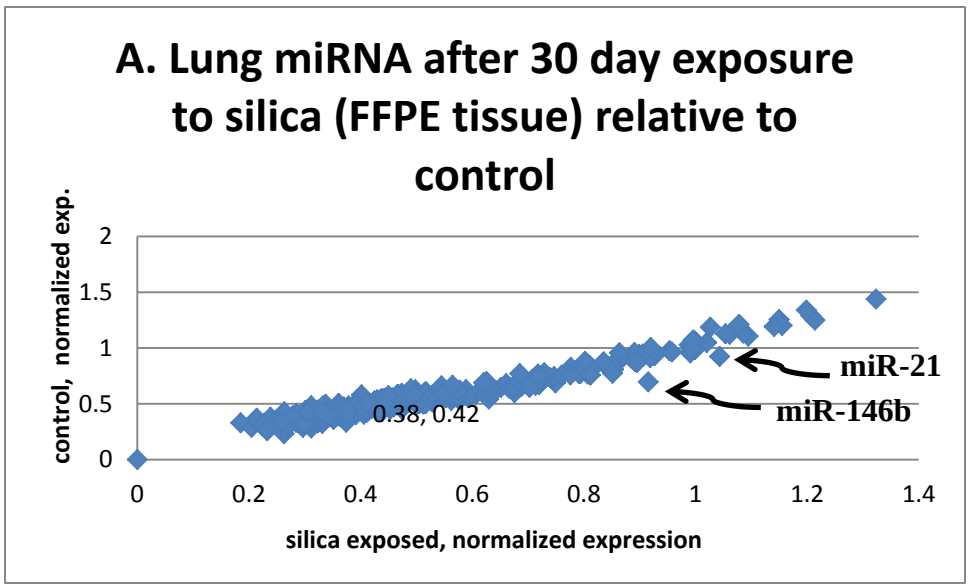

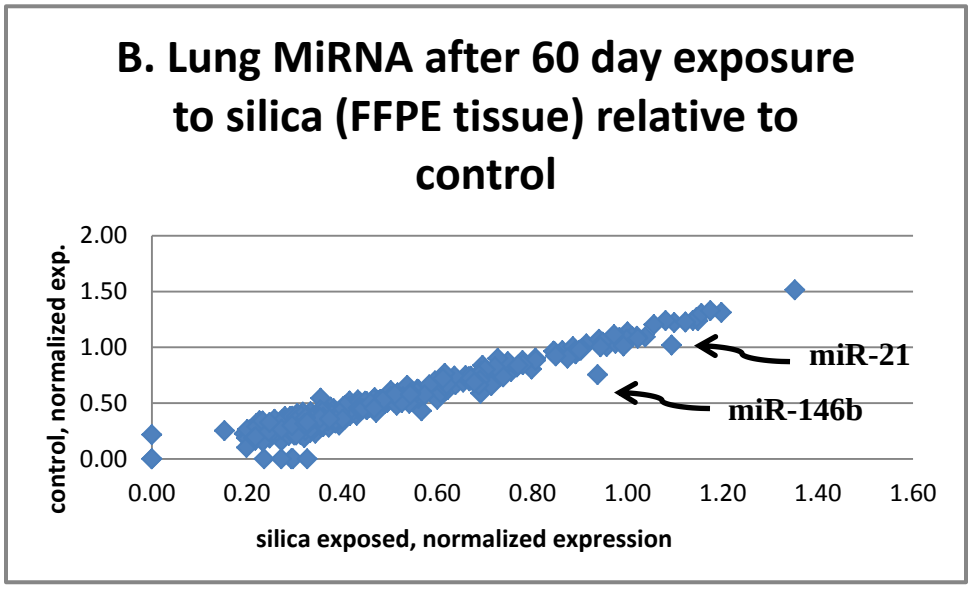

Figure 1. MiRNA expression from lungs of silica exposed animals as a function of control expression. *(A)* MiRNA data from 5 control lung samples plotted as a function of 5 silica-exposed lung samples, 30 days of exposure. *(B)* MiRNA data from 3 control lung samples plotted as a function of 4 silica-exposed lung samples, 60 days of exposure. MiRNAs 21 and 146b emerged as strongly up-regulated after both exposure periods.

Since 3 to 5 lung samples were profiled for each condition, a separate data reduction workflow permitted the calculation of p values for each miRNA. The miRNAs that were differentially expressed up or down more than 1.7-fold and with a p value of 0.06 or lower after 30 days of exposure are given in Supplementary Tables 1 & 2. Supplementary Table 3 lists miRNAs up-regulated after 60 days of exposure. Combining these findings, Table 5 shows that ten miRNAs including miR-146b and miR-21 were differentially expressed and independently detected at both 30 days and 60 days.

We also profiled several samples twice (technical replicates) as an assessment of the reproducibility of this profiling method. Correlation coefficients of technical replicates were quite high as shown in Supplementary Figure 2.

Table 5. miRNAs up-regulated in lungs dosed with 10mg/kg silica, after both 30 and 60 days of exposure (fold-upregulation >1.7; p <0.06). miRNA, microRNA; si, silica treated; con, control or saline treated; d30, 30 days after saline or dust exposure; d60, 60 days after saline or dust exposure. See also Supplementary Tables 1, 2 & 3.

miRNA	si/con d30	si/con d60
652	2.4	1.9
146b	8.2	6.6
96	2.6	2.6
21	4.8	2.9
101b	2.8	1.9
141	3.2	1.5
17-5p	2.3	1.6
146a	2.7	1.7
224	1.9	2.1
223	2.4	1.9

Lung miRNA are compared to differentially expressed miRNAs from BALF or serum after dosing with IR8, IR9 dusts or silica in Supplementary Table 4. This represents a master listing of differentially expressed miRNAs from the rat dust instillation model that can serve as a guide when miRNAs are profiled from the STAMPEDE clinical samples. Some of the miRNAs listed in Supplementary Table 4 are more reliable because biological replicate samples were studied (lung) or because the miRNAs were measured by two independent methods (day 60, silica dosed at 5 mg/kg and 10 mg/kg). The serum results are the least reliable because of the finding of hemolysis as discussed in the 2012 Annual Report. Overall, the finding that many miRNAs were detected in the lung such as 146a, 23a, 21, 200a, 223, 200c, and 200b that were also previously found in BALF or serum validates the earlier findings. Perhaps not surprisingly, miRNAs such as 21, 23, 146a, 146b, 141, 429, 200a, 200b, and 200c that were often detected in this study from lung, BALF or serum have been associated with lung or other pathologies.

MiRNAs and lung pathology: Discussion

We have profiled miRNAs from fixed, embedded lung tissue derived from the study 1 animals. Here we concentrated on the animals that were challenged with 10 mg/kg silica after 30 and 60 days, since these groups yielded interesting profiles in lavage fluid as well as notable pathology. We detected a group of miRNAs that were up-regulated in both lavage fluid and in lung tissue: miRNAs 21, 146a, 146b, 141, and 200b. By profiling multiple lung tissue samples we were able to apply Welch's T test and calculate p values as an objective assessment of the reliability of these observations. The p values of these miRNAs varied from 0.001 to 0.01, in the range of highly significant. The simple fact that a consistent group of miRNAs are found both in lung and lavage suggests that these miRNAs are produced in the lung and shed into the lavage fluid. This possibility strengthens the designation of this group as candidate biomarkers. It is also significant that certain miRNAs that tended to be detected together such as miR 200b, 200c, and 429 are in fact coordinately expressed since they are derived by processing from the same primary transcript[28]. Other miRNAs from the current study that are expressed from the same genes include 200a with 141 and 146a with 146b. These relationships are shown in Table 6 that also

compares the key miRNA candidate markers from the dust instillation study with other lung diseases. Consistent with a role in lung pathology, miRNAs 223, 21, and the 200b/200c/429 and 200a/141 clusters have also been reported in allergic inflammation[23] and the 200bc429 and miR21 were reported in idiopathic pulmonary fibrosis[11]. These findings are summarized in Table 6.

That these results from lung confirm the results from lavage fluid also invites a more detailed investigation of possible mechanistic contributions of these miRNAs to the cellular changes that were noted by the pathologists. For example the pathologists reported hyperplastic changes in the pulmonary epithelium at 30 to 60 days. Granuloma formation in this dust instillation model was reported in the pathology report and an example is reproduced below as Supplementary Figure 3 (ref. 22). MiRNA-21 has repeatedly been associated with proliferative phenomena. MiR-21 and miRNAs of the 200 family have been linked to differentiation of epithelial cells into mesenchymal fibroblasts or the epithelial-to-mesenchymal transition (EMT), a driving mechanism that can contribute to pulmonary fibrosis. Interstitial fibrosis in response to dust instillation was documented in the pathology report and an example is reproduced below as Supplementary Figure 4 (ref. 22).

Many of the miRNA candidates identified in the rat dust instillation model have been linked to diseases in humans and in some cases to particular biological processes that contribute to those diseases. MiR-21 was identified in BALF and subsequently confirmed in lung tissue at longer exposure stages when alveolitis, granuloma formation, and interstitial fibrosis after silica treatment were noted in the pathology report[22].

Table 6. miRNAs up-regulated in dust instillation study compared with other conditions**.**

miRNA species or group	Lung, silica[1]	BALF, IR8 dust[2]	BALF, silica[2]	Allergic inflammation[23]	Fibrotic lung disease[11]
200bc429	x	x	x	x	x
200a141	x	x	x	x	
21	x	x	x	x	x
223	x	x	x	x	
669b		x	x		
146a	x		x		

Legend: Note 1: miRNA from Tables 5 & Supplementary Tables 1-3. Note 2: from Supplementary Table 4.

A role for this miRNA has emerged in the cell differentiation changes that occur normally during development, but also reoccur when adult tissues are wounded or stressed: the processes of EMT and the endothelial-to-mesenchymal transition. An EMT could certainly contribute to some or some or all of the formation of the granulomas and interstitial fibrosis noted in the lungs of the silica-treated rats. MiR-21 has been identified as a positive regulator of EMT, since it is up-regulated by TGFβ and it acts to reduce expression from the mRNA of the proto-oncogene phosphatase and tensin homolog (PTEN) which is a negative regulator of EMT. PTEN itself normally helps repress the Akt/PKB pathway which has been implicated in initiating EMT[24]. Perhaps because of its actions to modulate proto-oncogenes, miR-21 has emerged as a marker for both lung and prostate cancer. In a case-control study, serum levels of miR-21 were elevated

in patients with non-small cell lung cancer compared to age-matched controls ($p<0.01$) and ominously, lung cancer patients with the highest circulating miRNA-21 levels had the shortest life expectancy[25]. MiR-21also has biomarker utility in prostate cancer where the level of this miRNA was elevated in patients with hormone-refractory prostate cancer ($p=0.012$). MiR-21 levels also correlated closely to prostate specific antigen levels in the serum before chemotherapy and after PSA levels declined in response to chemotherapy[26]. Since miR-21 was higher in patients who were resistant to docetaxel-based chemotherapy, the authors suggested that miR-21 serum levels could be used as a marker to indicate transformation to hormone refractory disease and thus be a potential predictor for the efficacy of this particular chemotherapy. MiR-21 and its target PTEN have also been implicated in hepatocellular carcinoma[27]. Inhibition of miR-21 in cell lines derived from hepatocellular carcinoma led to increased expression of PTEN and reduced cell proliferation, migration and invasion. Enhanced expression of miR-21 increased cell proliferation, migration, and invasion. These studies show that serum levels of miR-21 can be a biomarker for diseases such as cancer, and it can stratify one type of cancer on the basis of drug-resistance. Given that miR-21 is produced at many sites in the body in response to common processes such as fibrosis and cancer its value as a single marker is limited. But it could be quite valuable in a panel of markers that focus on a particular pathology, disease, or tissue.

Roles in EMT have also been described for the miR-200bc/429 and 200a/141 groups (Table 6), where they have been proposed to modulate the levels of Zeb1 and Zeb 2, key transcription factors that maintain the epithelial state[28,29]. These miRNAs have been associated with breast cancer cell invasion, viability, apoptosis resistance and growth factor responses[28].

MiRNA profiling: conclusions

Two of the miRNAs that were found in lung tissue as well as BALF samples (miR-21, miR-146 family) have been associated with disease processes, including disorders of the lung. This work can be extended to identify miRNAs in preserved tissue that are associated with particular pathologies if desired. The overall method should be accessible to other labs since it uses commercially available techniques and equipment. The results confirmed several of the candidate miRNAs we had previously documented in lavage fluid. While many of these miRNAs are now associated with silica-induced lung disease, they are probably not lung-specific. Many of the miRNAs we detected have also been reported in the blood or from the affected organs in pre-clinical models of other diseases with strong components of cell proliferation or inflammation. Nonetheless, the approach outlined here can link archived tissue that harbors a particular pathology with a characteristic molecular profile. In combination with other markers such as proteins, they may contribute information about lung pathology.

Analysis of STAMPEDE samples in progress

ISB and PNNL are starting to study samples of BALF, blood serum, and urine that were collected from soldiers with dyspnea. We are collaborating with Dr. Michael Morris at the Brooke Army Medical Center, San Antonio, Texas who collected the clinical specimens from active duty soldiers with some type of breathing disorder who enrolled in Dr. Morris' registry and clinical program called the 'Study of Active Duty Military for Pulmonary Disease Related to Environmental Dust Exposure' (STAMPEDE). Soldiers who enrolled in STAMPEDE received complete pulmonary examinations and gave samples of blood, BALF and urine. ISB received complete sample sets from 47 subjects and a sample of blood and urine (but no BALF) from a forty-eighth subject. The plan forward is to submit the 48 urine samples and 47 BALF samples for complete proteomics analysis. In addition microRNAs will be profiled in 48 urine samples, 48 blood samples, and 47 BALF samples. As of January, 2013 Dr. Morris' clinic has started collecting control samples from age-matched soldiers with no dyspnea or other known lung disease.

Key Research Accomplishments

- A list of proteins that were released into BALF by IR8 dust at different exposure periods. These proteins represent candidate biomarkers of the observed lung pathology, subject to additional validation studies; see Table 1.
- A list of proteins that were released into BALF by silica at different exposure periods. These proteins represent candidate biomarkers of the observed lung pathology, subject to additional validation studies; see Table 2.
- A list of proteins that were released into BALF by both IR8 dust and silica at different exposure periods; see Table 3.
- A list of miRNA species that showed increased levels in BALF by silica at late exposure periods. These miRNAs are candidate biomarkers of the observed lung pathology, subject to additional validation studies; see Supplementary Table 4.
- A list of miRNA species detected in BALF or serum, evoked in response to dust or silica, that have been validated after detection in the lung and in other studies of lung disease. These miRNAs are candidate biomarkers of the observed lung pathologies, suitable for comparison to human clinical samples; see Table 6.
- A method to profile miRNA from formalin-fixed paraffin-embedded tissue sections. This permits investigation of the association of particular miRNAs with discrete cellular pathologies in legacy samples.

Reportable Outcomes

- *Preliminary results from this study were presented at a meeting of the Pulmonary IPR Workgroup, 1-2 December 2011, convened by USACEHR and held at Fort Detrick MD.*
- *Studies in the second year of this study were presented at a meeting of the Pulmonary IPR group convened by MOMRP, 3 December 2012.*
- *A manuscript that presents the combined proteomics and miRNA analysis of BALF is in preparation. This paper will be submitted to an open access journal.*
- *At the time of any publication, proteomics findings and miRNA findings will be submitted to the appropriate public databases*

Overall conclusions

This study applied highly sensitive methods to identify proteins and miRNAs that changed in BALF at the same time as known pathologic processes were active in the lung. The proteins and miRNAs we listed thus represent candidate markers of these processes, such as granuloma formation or active fibrosis. Verification of these results in the same or a related pre-clinical model would be one logical next step. Finally, validation of any candidate markers can only be accomplished by testing with human clinical specimens. Some of the strongest data we reported may be the proteins and miRNAs that are shed into the BALF late after exposure to silica. These molecules, such as miR-200s, may be linked to the tissue remodeling characteristics of granuloma formation that were discussed in the pathology report on this model. Such markers have not yet been reported and these findings may be a welcome addition to the literature on inhalation toxicology.

References

1. Brown, J.N., et al. Characterization of Macaque Pulmonary Fluid Proteome during Monkeypox Infection: Dynamics of Host Response. Mol Cell Proteomics (2010).

2. Brown, J.N., et al. Macaque Proteome Response to Highly Pathogenic Avian Influenza and 1918 Reassortant Influenza Virus Infections. J Virol (2010).

3. Adkins, J.N., et al. A proteomic study of the HUPO Plasma Proteome Project's pilot samples using an accurate mass and time tag strategy. Proteomics 5, 3454-3466 (2005).

4. Kim, S., Gupta, N. & Pevzner, P.A. Spectral probabilities and generating functions of tandem mass spectra: a strike against decoy databases. J Proteome Res 7, 3354-3363 (2008).

5. Jaitly, N., et al. Decon2LS: An open-source software package for automated processing and visualization of high resolution mass spectrometry data. BMC Bioinformatics 10, 87 (2009).

6. Monroe, M.E., et al. VIPER: an advanced software package to support high-throughput LC-MS peptide identification. Bioinformatics 23, 2021-2023 (2007).

7. Stanley, J.R., et al. A statistical method for assessing Peptide identification confidence in accurate mass and time tag proteomics. Anal Chem 83, 6135-6140 (2011).

8. Nesvizhskii, A.I., Keller, A., Kolker, E. & Aebersold, R. A statistical model for identifying proteins by tandem mass spectrometry. Anal Chem 75, 4646-4658 (2003).

9. Polpitiya, A.D., et al. DAnTE: a statistical tool for quantitative analysis of -omics data. Bioinformatics 24, 1556-1558 (2008).

10. Price N, Trent J, El-Nagar A, Cogdell D, Taylor E, et al 2007. Highly accurate two-gene classifier for differentiating gastrointestinal stromal tumors and leiomyosarcomas. Proc. Natl. Acad. Sci. USA. doi: 10.1073/pnas.0611373104.

11. Cho J-H, Gelinas R, Wang, K, Etheridge A, et al. 2011. Systems biology of interstitial lung diseases: integration of mRNA and microRNA expression changes. BMC Medical Genomics. 4:8 doi:10.1186/1755-8794-4-8.

12. Henderson, R.F., Damon, E.G. & Henderson, T.R. Early damage indicators in the the lung I. Lactate dehydrogenase activity in the airways. Toxicol Appl Pharmacol 44, 291-297 (1978).

13. Wu, W., Patel, K.B., Booth, J.L., Zhang, W. & Metcalf, J.P. Cigarette smoke extract suppresses the RIG-I-initiated innate immune response to influenza virus in the human lung. Am J Physiol Lung Cell Mol Physiol 300, L821-830 (2011).

14. Drent, M., Cobben, N.A., Henderson, R.F., Wouters, E.F. & van Dieijen-Visser, M. Usefulness of lactate dehydrogenase and its isoenzymes as indicators of lung damage or inflammation. Eur Respir J 9, 1736-1742 (1996).

15. Abboud, R.T. & Vimalanathan, S. Pathogenesis of COPD. Part I. The role of protease-antiprotease imbalance in emphysema. Int J Tuberc Lung Dis 12, 361-367 (2008).

16. Hara, H., et al. Involvement of Creatine Kinase B in Cigarette Smoke Induced-Bronchial Epithelial Cell Senescence. Am J Respir Cell Mol Biol (2011).

17. Meloni, F., et al. Bronchoalveolar lavage fluid proteome in bronchiolitis obliterans syndrome: possible role for surfactant protein A in disease onset. J Heart Lung Transplant 26, 1135-1143 (2007).

18. De Dooy, J.J., Mahieu, L.M. & Van Bever, H.P. The role of inflammation in the development of chronic lung disease in neonates. Eur J Pediatr 160, 457-463 (2001).

19. Mangum, J., Bermudez, E., Sar, M. & Everitt, J. Osteopontin expression in particle-induced lung disease. Exp Lung Res 30, 585-598 (2004).

20. Sabo-Attwood, T., et al. Osteopontin modulates inflammation, mucin production, and gene expression signatures after inhalation of asbestos in a murine model of fibrosis. Am J Pathol 178, 1975-1985 (2011).

21. Zhou, Y., Murthy, J.N., Zeng, D., Belardinelli, L. & Blackburn, M.R. Alterations in adenosine metabolism and signaling in patients with chronic obstructive pulmonary disease and idiopathic pulmonary fibrosis. PLoS ONE 5, e9224 (2010).

22. Green, FHY and Harley R. 2011. Report to the National Institute for Occupational Safety and Health on the lung pathology in rats exposed to intratracheal injections of respirable sized dusts from Iraq. Final report; December 16, 2011(unpublished).

23. Lu, T. 2012. MiRNAs associated with lung inflammation (Thesis abstract); University of Cincinatti

24. Kumarswamy R, Volkman I, Thum T. 2011. Regulation and function of miRNA-21 n health and disease. *RNA Biology* 8:5 706-713. Doi: 10.4161/rna.8.5.16154.

25. Wang Z, Bian H, Wang J, Cheng Z, et al 2011. Prognostic significance of serum miRNA-21 expression in human non-small cell lung cancer. *J Surgical Oncology* 104: 847-851. Doi:10.1002/jso.22008.

26. Zhang H, Yang L, Zhu Y, Yao X, Zhang S, Dai B et al. 2011. Serum miRNA-21: elevated levels in patients with metastatic hormone-refractory prostate cancer and potential predictive factor for the efficacy of docetaxel-based chemotherapy. The Prostate 71: 326-331; doi: 10.1002/pros.21246.

27. Meng F, Henson R, Wehbe-Janek H, Ghoshal K, Jacob S, Pate T. 2007. MicroRNA-21 regulates expression of the PTEN tumor suppressor gene in human hepatocellular cancer. Gastroenterology 133: 647-658. Doi: 10.1053/j.gastro.2007.05.022

28. Uhlmann S, Zhang J, Schwager A, Mannsperger H, et al. 2010. miR-200bc/429 cluster targets PLCgamma1 and differentially regulates proliferation and EGF-driven invasion than miR-200a/141in breast cancer. Oncogene 29:4297-4306. Doi:10.1038/onc.2010.201

29. Braken C, Gregory P, Koleshikoff N, Bert A et al. 2008. A double-negative feedback loop between ZEB1-SIP1 and the mircoRNA-200 fmaily regulates epithelial-mesenchymal transition. Cancer Res. 68: 7846-7854. Doi:10.1158/0008-5472.CAN-08-1942

Supplementary Data

Supplementary Table 1. miRNAs increased in lungs by silica after 30 days.

	miRNA	p value	Si/control
1	rno-miR-652	0.001	2.4
2	rno-miR-146b	0.001	8.2
3	rno-miR-19a	0.003	2.5
4	rno-miR-17-5p	0.003	2.3
5	rno-miR-101b	0.004	2.8
6	rno-miR-141	0.004	3.2
7	rno-miR-21	0.004	4.8
8	rno-miR-146a	0.007	2.7
9	rno-miR-200b	0.009	2.4
10	rno-miR-16	0.010	2.1
11	rno-miR-223	0.011	2.4
12	rno-miR-199a-3p	0.012	2.2
13	rno-miR-429	0.012	2.2
14	rno-miR-27b	0.015	2.2
15	rno-miR-96	0.016	2.6
16	rno-miR-20a+rno-miR-20b-5p	0.017	2.0
17	rno-miR-152	0.020	2.1
18	rno-miR-29c	0.022	2.0
19	rno-miR-98	0.024	2.1
20	rno-miR-142-3p	0.029	2.1
21	rno-miR-224	0.041	1.9

Legend: miRNAs differentially expressed 1.9-fold or greater with p values 0.05 or lower from FFPE lung tissue after 30 days exposure from rats treated with 10 mg/kg silica.

Supplementary Table 2. miRNAs decreased in lungs by silica after 30 days.

	miRNA	p value	Si/control
1	rno-miR-411	0.009	0.4
2	rno-miR-1912-5p	0.016	0.5
3	rno-miR-154	0.025	0.4
4	rno-miR-297	0.025	0.4
5	rno-miR-343	0.028	0.5
6	rno-miR-3563-3p	0.038	0.5
7	rno-miR-770	0.046	0.4
8	rno-miR-760-5p	0.050	0.5
9	rno-miR-343	0.028	0.5

Legend: miRNAs differentially expressed 0.5-fold or less with p values 0.05 or lower from FFPE lung tissue after 30 days exposure from rats treated with 10 mg/kg silica.

Supplementary Table 3. miRNAs increased in lungs by silica after 60 days.

miRNA	p value	silica/control
rno-miR-183	3.4E-05	2.6
rno-miR-146b	0.001	6.6
rno-miR-96	0.002	2.6
rno-miR-21	0.004	2.9
rno-miR-101b	0.013	1.9
rno-miR-652	0.019	1.9
rno-miR-3584-3p	0.020	2.2
rno-miR-144	0.029	0.5
rno-miR-326	0.029	1.5
rno-miR-146a	0.030	1.7
rno-miR-224	0.032	2.1
rno-miR-17-5p	0.032	1.6
rno-miR-17-2-3p	0.037	1.8
rno-miR-223	0.037	1.9
rno-miR-340-5p	0.038	1.4
rno-miR-200c	0.044	1.6
rno-miR-3558-5p	0.044	1.6
rno-miR-92a	0.045	1.6
rno-miR-875	0.048	1.6
rno-miR-18a	0.049	1.8
rno-miR-3553	0.055	1.7
rno-miR-141	0.060	1.5

Legend: miRNAs differentially expressed 1.5-fold or more with p values 0.06 or lower from FFPE lung tissue after 60 days exposure from rats treated with 10 mg/kg silica.

Supplementary Table 4. Differentially expressed miRNAs from study 1 & 2.

miRNA species	Study 1:lung d30+d60, silica10 (note 5)	Study 1: BALF, d60,silica 5 (note 1)	Study 1: BALF, d60, silica 10 (note 2)	Study 1:BALF, d60, IR8 10 (note 3)	Study 2: BALF, d150, IR9 med (note 4)	Study 2: BALF, d150, NIST med (note 4)	Study 1: serum, d60+120, silica 10 (note 6)
361		x					
628		x					
378		x					x
146a	x	x					x
30a		x					x
1224		x					x
125a-5p		x					x
290;466;208		x					x
let-7b		x			x		
181a		x			x		
23a		x (2 methods)	x	x	x		
21	x	x (2 methods)	x	x	x		x
200a		x (2 methods)	x	x			
223	x		x	x	x		
669b			x	x	x	x	
29a					x		
34c					x		
34b-5p					x		
429	x				x		
23b					x		
200c	x				x		
200b	x				x		
150					x		
210					x		
151-5p					x		
93					x		
7c					x		
30b					x		
99b					x		
375					x		
205					x		
29c					x		
30c					x	x	
652	x						
146b	x						
19a	x						
17-5p	x						
101b	x						
141	x						
16	x						
199a-3p	x						
27b	x						

96	x					
20a+20b	x					
152	x					
29c	x					
98	x					
142-3p	x					
224	x					
411	x					
1912-5p	x					
154	x					
297	x					
343	x					
3563-3p	x					
770	x					
760-5p	x					
343	x					
183	x					
3584-3p	x					
144	x					
326	x					
17-2-3p	x					
340-5p	x					
3558-5p	x					
92a	x					
875	x					
18a	x					
3553	x					
466c						x
122						x
451						x

Legend: Note 1: miRNA from BALF, day 60, 5 mg/ml silica, Table 8 & 9 2012 Annual Report; Note 2: miRNA from BALF, day 60, IR8 dust 5 mg/ml; Note 3: BALF, d60, , Note 4: study 2, IR9 or NIST dusts, medium dose, 120+150 day exposure (assay by hybridization); Note 5: study 1, miRNA from FFPE lung tissue, d30+d60, silica 10 mg/ml, this report, Tables 1-3; Note 6: study 1, serum, d60+d120; silica 10 mg/ml (assay by hybridization).

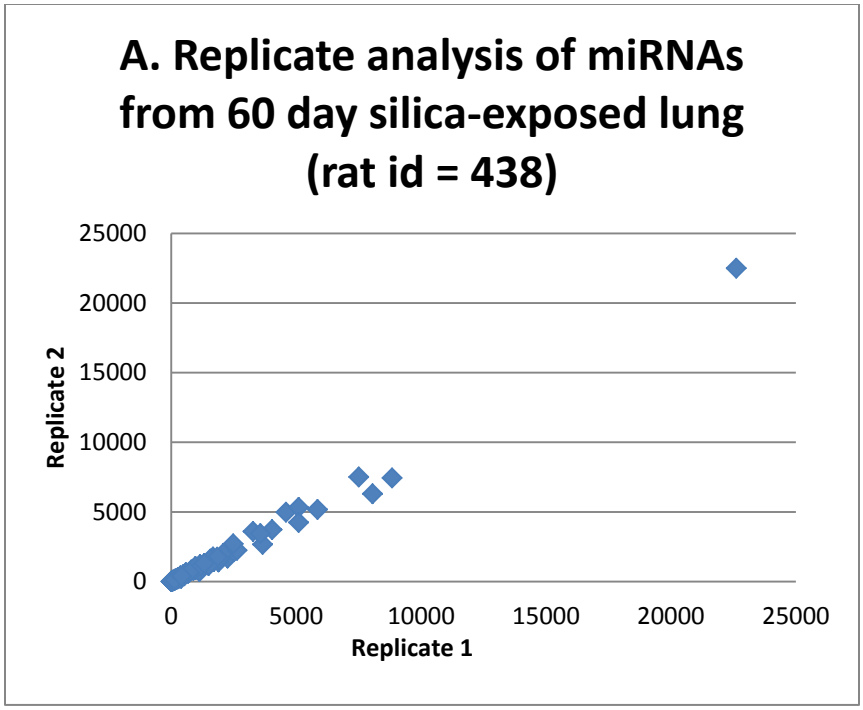

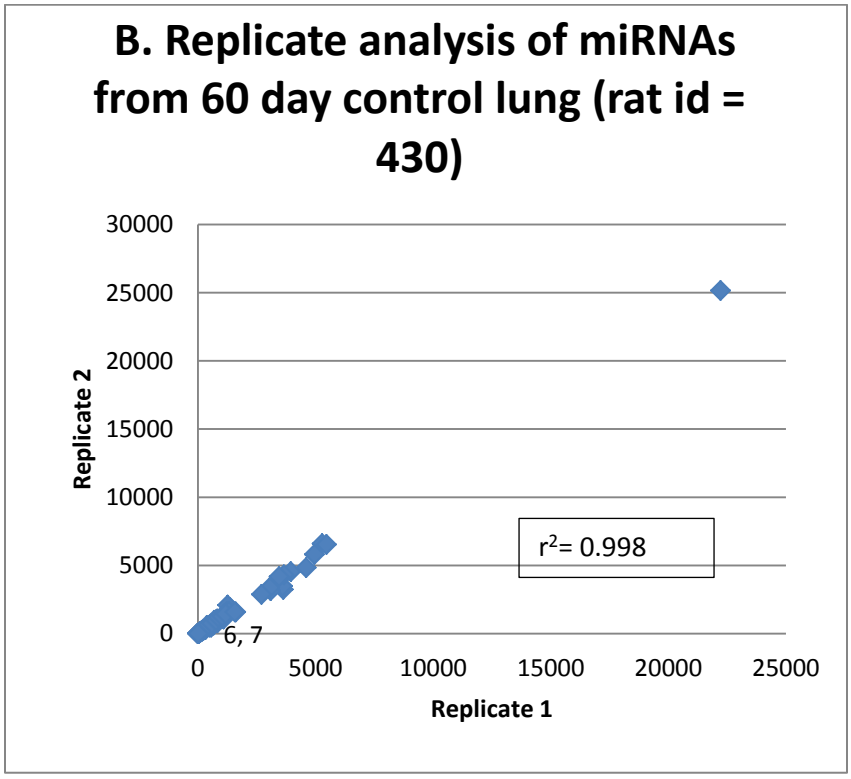

Supplementary Figure 2. Similarity of miRNA values from the same lung RNA sample. A. Technical replicate values from 167 miRNAs from rat 438 plotted against one another; r^2=0.995. B. Technical replicate values from 135 miRNAs from rat 430 plotted against one another; r^2=0.998.

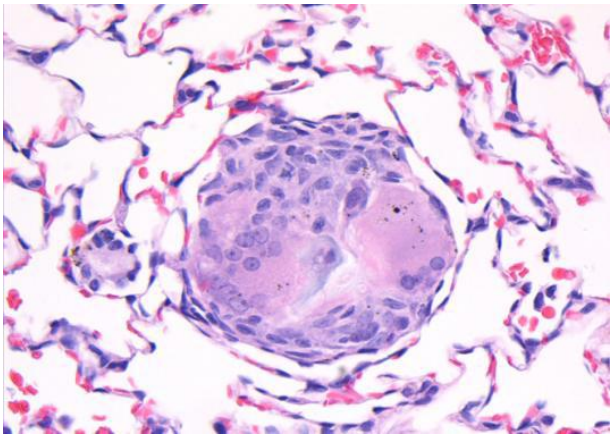

Supplementary Figure 3. Typical granuloma from rat lung. *"Occasional granulomas, often of foreign body type, were seen in the lung parenchyma for all dusts. The lowest gradings were recorded for the IR8 and IR9 dusts. Silica, NIST and P15 dusts all had similar scores for granulomas in the lung parenchyma. MiRNA expression in BALF from rats treated with 10 mg/ml IR8 dust or silica relative to controls at the indicated times*". Photo id: F:\ Iraq dust II photos\314 RD 40x gran.jpg; from pathology report by Francis Green & Russell Harley, reference 22.

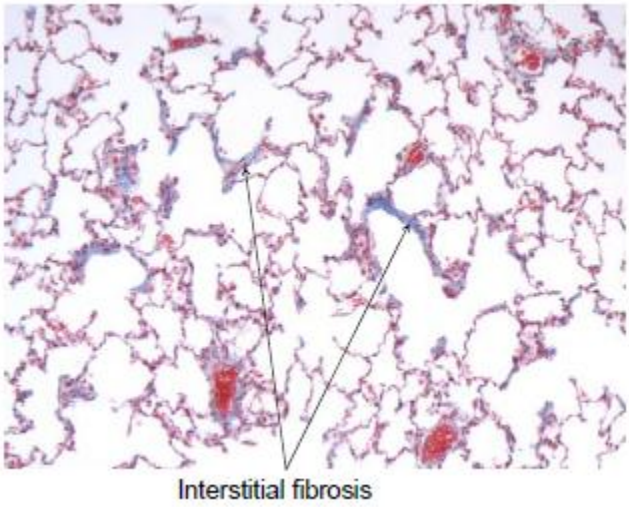

Supplementary Figure 4. Interstitial fibrosis from rat lung. *"This feature was defined as the laying down of collagen and/or reticulin or elastic tissue within the interstitium of the lung. The interstitium in this context generally refers to the gas exchange portions of the lung. Although this feature can be readily identified on H&E stained sections, it is best seen from a quantitative point of view with the Trichrome stain. None of the dusts scored particularly highly for interstitial fibrosis. Silica dust was slightly more fibrogenic than the Iraq or NIST dusts and showed a temporal and dose-response relationship…" F*rom the pathology report by Francis Green & Russell Harley, reference 22.

Personnel receiving salary support on this contract:

At the Institute for Systems Biology

1. Richard Gelinas
2. Kai Wang
3. Sara McClarty
4. Ji-Hoon Cho

At Pacific Northwest National Laboratory

1. Dr. Joseph Brown
2. Dr. Josh Adkins
3. Nancy Colton
4. Charles Ansong